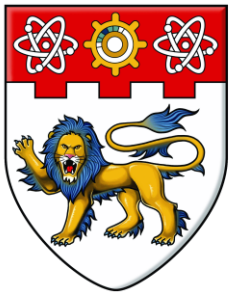

NANYANG TECHNOLOGICAL UNIVERSITY

MOLYBDENUM CARBIDE NANOWIRES AS EFFICIENT HETEROGENEOUS CATALYST FOR CO_2 HYDROGENATION

WU YUE

School of Chemical and Biomedical Engineering

2016

MOLYBDENUM CARBIDE NANOWIRES AS EFFICIENT HETEROGENEOUS CATALYST FOR CO_2 HYDROGENATION

WU YUE

School of Chemical and Biomedical Engineering

A thesis submitted to the Nanyang Technological University

in fulfillment of the requirement for the degree of

Master of Engineering

2016

Acknowledgement

This thesis work was made in School of Chemical and Biomedical Engineering (SCBE) at Nanyang Technological University.

I would like to thank my supervisor, Prof Liu Bin, for giving me the opportunity to perform my thesis work, and for the support and positive motivation during the work.

Also, I would like to express my sincere thanks to Dr Yang hongbin, Dr Dai yihu, Dr Gaojiajian, Mr Gong heqing, Mr Yan yong for your help with my experiments and analyses.

Last but not least, I would like to extend my appreciation to my family, who have been there for me in times of good and bad, and been a constant support for me in my pursuits.

Abstract

CO_2 hydrogenation is one of the various strategies for CO_2 reduction. Molybdenum carbide is one of the heterogeneous catalysts that have been found catalytically active for CO_2 hydrogenation. From the open literature, catalytic performance of molybdenum carbide catalyst is linked with their crystal structure. However the characteristic properties of different crystal structures still deserve further investigation. In this research, two main phases of molybdenum carbide catalysts, α-MoC_{1-x} and β-Mo_2C were synthesized for investigation. The conversion of α-MoC_{1-x} into active α phase was achieved by slightly elevate the carburization temperature from 700℃ to 720℃. The catalytic activity of these molybdenum carbide nanowires materials was assessed in the hydrogenation of CO_2. Result showed the apparent activity of active α-MoC_{1-x} catalyst synthesized at 720℃ were 10% higher than β-Mo_2C due to its 4 times larger surface area, however the intrinsic activity of active α-MoC_{1-x} catalyst is still lower than β-Mo_2C catalyst. With In-situ XPS technique, we discovered the reducibility of β-Mo_2C was significantly higher than α-MoC_{1-x}, which corresponded to β-Mo_2C catalyst high intrinsic activity. We then conclude the reducibility difference, closely linked to crystal structure difference, and strongly affected the catalytic performance. DRIFTS was used to study the adsorption properties of molybdenum carbide nanowires catalyst. We proposed the weak adsorption of CO on molybdenum carbide catalyst explained catalyst's high selectivity behavior.

Table of contents

List of Tables, Figures and Illustrations

List of Symbols, Abbreviations and Nomenclature

AHM	Ammonium heptamolybdate tetrahydrate $(NH_4)_6Mo_7O_{24} \cdot 4H_2O$
a.u	Arbitrary units
BET	Brunauer-Emmett-Teller (surface area)
Ea	Activation energy
EDX	Energy Dispersive X-ray Spectroscopy
HRTEM	High Resolution Electron Microscopy
SEM	Scanning Electron Microscopy
XPS	X-ray Photoelectron Spectroscopy
XRD	X-ray diffraction
α-MoC_{1-x}	Face centered cubic Molybdenum Carbide
β-Mo_2C	Hexagonal Molybdenum Carbide

1. Introduction

Human activities have strong effect on altering the earth carbon cycle by increasing the emission of CO_2 in the atmosphere.[1] The increasing CO_2 concentration will have significantly effect on the earth equilibrium environment. CO_2 hydrogenation to CO (RWGS reaction) has been regarded as one of the most favorable processes for CO_2 reduction.[2] In industry, with the development of Fischer–Tropsch synthesis, H_2 and CO as syngas can be utilized to produce long-chain hydrocarbons.[3] RWGS reaction is one of the most promising methods for CO production, and the design of the RWGS catalyst has attracted intensive attention.[2] Considering RWGS reaction is an endothermic reaction, high operating temperature is required and the use of an efficient catalyst capable of withstanding high temperatures and being selective to CO during the RWGS reaction is necessity.

Precious metals are traditional active heterogeneous catalysts in RWGS reaction due to precious metals are highly active for H_2 dissociation.[4] However, precious metal has low abundance, which is not suitable for large-scale industrial processes.[5] These days, Pt-like materials, which are composed of cheap and widely distributed elements, have been developed as alternative catalysts to replace precious metals.[6]

Molybdenum carbides have been regarded as the most favorable alternative catalysts to replace precious metals, due to their analogical electronic properties to Pt.[7] In the particular case of hydrogenation reactions, molybdenum carbide (Mo_2C) has been studied

for over 40 years for its potential as a hydrogenating catalyst. Since Levy et al. reported the Pt-like behavior of tungsten carbide.[8] As a catalyst for CO_2 to CO conversion, Chen et al reported that Molybdenum carbide catalyst even outperform monometallic Pt, Pd and Pt-Co, Pd-Co bimetallic catalysts.[9]

Utilizing Mo_2C nanowires in RWGS reaction is highly attractive, with organic-inorganic method, the as-obtained Mo_2C nanowires are formed small nanoparticles with large reactive surface area, leading to their superior activity. On the other hand, catalytic performance of molybdenum carbide catalysts is linked with their crystal structure. Even though molybdenum carbides catalysts with different phases have been studied and developed for various applications, the characteristic properties of different crystal structure still have not been fully understood. And also, molybdenum carbide catalyst's high selectivity behavior also not explained from the open literature.

1.1. Aims and objectives

1.1.1. Aims

The aims of this thesis are to gain a better understanding of the RWGS reactions, develop active and stable molybdenum carbide nanowires catalysts for CO_2 hydrogenation to CO, and investigate the characteristic properties of different crystal structure.

1.1.2. Objectives

Two main phases of molybdenum carbide catalysts, α-MoC_{1-x} and β-Mo_2C were synthesized for RWGS reaction. Three mix phases of α-MoC_{1-x} and β-Mo_2C were also synthesized for evaluate the catalytic performance. Several characterization techniques were utilized to study the structure, surface properties and CO_2/CO adsorption of the catalysts.

2. Literature review

2.1. Catalytic hydrogenation of CO_2 to CO

Reducing CO_2 emissions has been at the heart of countless research over the past 20 years.[10] Utilizing CO_2 as feedstock is highly desirable in several potential energy-producing applications, it can not only reduce the concentration of CO_2 but also provides opportunities for industrial development.[11]

CO_2 is a thermodynamically stable molecule. Therefore, breaking the C=O bond requires high energy. In order to do so industrially, high temperatures, hydrogen and catalysts are required. These demands are what limit the use of CO_2 as an efficient carbon source in the industrial field.[12]

Several ways to sever the C=O bond exist. Electrocatalytic reduction of CO_2 has been achieved at room temperature and pressure using carbon supported Pt nanoparticles.[13] However, high electrical requirements limit the current use of the

electrocatalytic reduction of CO_2. Other methods like, photochemical reduction,[14] electrochemical reduction,[15] and use of enzymes,[16] to reduce CO_2 are small scale developing technologies which limit their industrialization potential.

Hydrogenation of CO_2 has been extensively studied recently in the wake of developments in catalysis surface science, nanotechnology and biology. Hydrogen contains intensive high energy and can be used as raw material for CO_2 reduction. One of hydrogen's key problematic in developing hydrogen economy is hydrogen storage and transportation. The reaction products of CO_2 hydrogenation will convert from gas to liquid fuels and hydrocarbons, such as methanol and DME, methane, all of them are easy for storage and transportation, and also they are remarkable components in internal combustion engines,.[17]

CO_2 hydrogenation to CO (RWGS reaction) has been regarded as one of the most favorable processes for CO_2 reduction. In industry, with the development of Fischer–Tropsch synthesis, H_2 and CO as syngas can be utilized to produce long-chain hydrocarbons.[18] RWGS reaction is one of the most promising methods for CO production, and the design of the RWGS catalyst has attracted intensive attention.

Considering RWGS reaction is an endothermic reaction, high operating temperature is required and the use of an efficient catalyst capable of withstanding high temperatures and being selective to CO during the RWGS reaction is necessity if the process is to be used industrially. The process requires standard equipment already available at most processing plants creating a good opportunity to industrialize the hydrogenation of

carbon dioxide through the RWGS reaction.

The selectivity of the catalyst is a requirement due to the nature of simultaneous side reactions occurring during the hydrogenation process. Among possible species being formed, methane is the most prominent. CH_4 is an undesired by-product for several reasons. First, the methanation processes require 4 H_2 molecules. In addition, natural gas prices will always be relatively low in comparison to the cost of H_2 manufactured from CH_4.

Instead of being considered a devil molecule, CO_2 could, with the proper initiative, become a strategic molecule in the processing industry. Further research dedicated to converting CO_2 to useful fuels parallel to the current research devoted to capturing the gas can reduce CO_2 emissions, and in the long term, reduce atmospheric CO_2 concentrations.

2.2. Theory of heterogeneous catalysis

This thesis focuses on heterogeneous catalysis, where the reactants originally is in the gas phase but reacts on the surface of a solid catalyst. Such catalysis relies on adsorption which is a phenomenon where molecules from the gaseous phase attach on to the solid surface. The fundamental principles behind adsorption originate from the thermodynamic driving force to decrease surface free energy. Strong adsorption involves molecular bond breakage when the new bonds between the reactants and the solid surface are created. This is called chemisorption in contrast to the weaker form of adsorption

without bond breakage called physisorption. Figure 1 shows the relationship between the two types of adsorption as a plot of the potential energy against the distance from a surface for two atoms and one molecule.[19] As expected the potential energy for the molecule (A_2) is zero far from the surface as it is unaffected by the attractive Can der Walls forces. Upon approaching the surface, it reaches a minimum due to increased electronic repulsion. In this dwell the molecule is physisorbed on the surface and can diffuse over long distances if the temperature is not too low. If the physisorbed molecule gains enough energy to approach the surface sufficiently close it can, depending on internal bond strength, either dissociate into atoms or chemisorb molecularly.

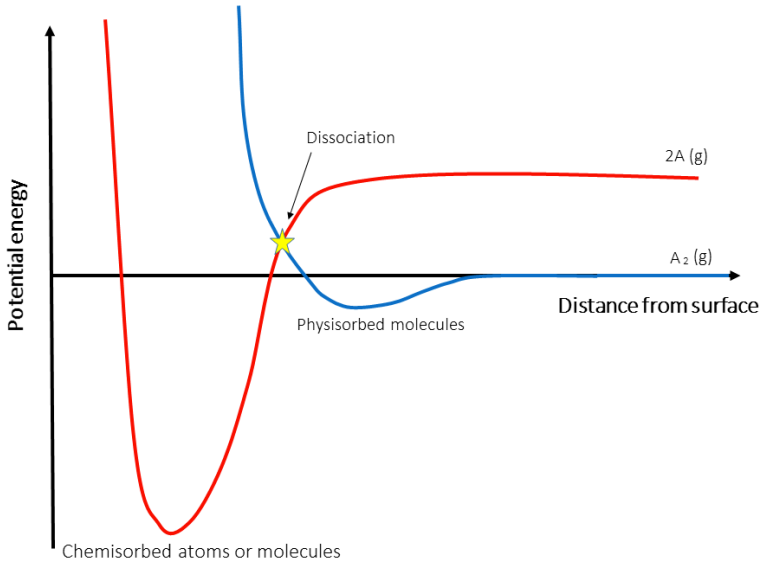

Figure 1. Energy path for atoms (red) and molecules (blue) approaching a surface.[19]

The chemical reaction efficiency can be improved by using an appropriate catalyst that lowers the barrier for the reaction (activation energy, Ea). In figure 2 the activation energy for a gas phase reaction is compared to that of a catalytic reaction.[19] It is clear that

the required energy to pass the barrier is lower when an appropriate catalyst is present. A catalytic reaction follows a catalytic cycle starting with reactant adsorption, followed by a surface diffusion and reaction and finally desorption of products into the gas phase. A simplified explanation of the surface reaction as being more efficient than a gas phase reaction is that the probability of the adsorbed species to collide when diffusing around on to the catalyst surface (two dimensional) is higher compared to gas molecules free to move in three dimensions. The results are formation of new molecules that could be desired products, unwanted products or intermediates. Creation of intermediates with otherwise unstable configuration is possible by stabilizing surface bonds. The total energy difference between reactants and products are however the same for the two reactions.

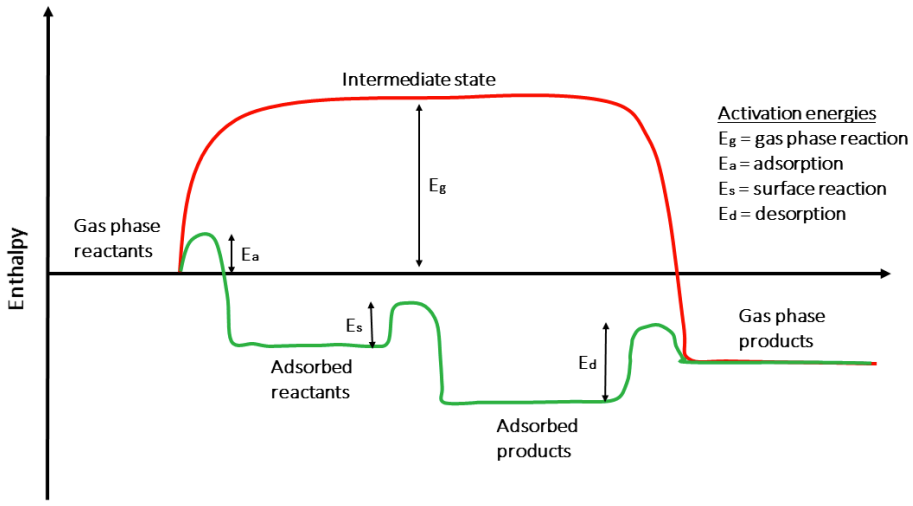

Figure 2. Plot of activation energies for an ordinary gas phase reaction (red) and the same reaction with an appropriate catalyst present (green).[19]

2.3. Common Catalysts for RWGS reaction

In order to predict the catalytic activity, Zigarnik et al demonstrated a methodology in which a computer program first determines a list of intermediate species for reactions.[20] Then they are able to calculate the activation energies of each step. They determined that the metals should yield the following order of catalytic activity based on kinetic simulations: Cu>Ni>Fe>Pt>Pd>Ag>Au.

Another way of predicting the efficiency of a catalyst for a specific reaction is to observe how it does in other similar reactions.[12] For instance, supported noble metals like Pt, Rh, Ru etc are known as good hydrogenation catalysts because of their capability to dissociate hydrogen. They could therefore show good activity for the RWGS reaction. In fact, several have tested Pt group metals for the RWGS reactions and have shown considerable conversion.[4]

It is well known that catalysts that are good for a forward reaction should also be good for the reverse reaction. The water gas shift (WGS) reaction has been thoroughly researched for decades. Several catalysts have been established as being efficient depending on the operating temperature. For instance low temperature (<350 ℃) WGS reactions often involve Cu-ZnO-Al_2O_3 catalysts while high temperature (>350 ℃) WGS reactions take place over Fe_2O_3-Cr_2O_3 catalysts.[21]

This section is dedicated to highlighting the most pertinent advances in catalysis relevant to the field of research. These include catalysts containing Pt, Cu, and Ni

catalysts.[22]

2.3.1. Cu catalyst for RWGS reaction

Copper (Cu) has been most prominently used in both steam reforming and in the WGS reaction. In fact, Cu has proven to be an effective catalyst for low temperature systems like the ones mentioned previously. Cu-based catalysts are very popularly studied in the RWGS reaction due to Cu catalysts are very active and favor CO formation during reaction[23],

Early research concerning hydrogenation of CO_2 over Cu metal catalysts was done using ZnO and Al_2Oe as a support. Work began on kinetic experiments attempting to understand the mechanism over a Cu based catalyst. The $CuO/ZnO/Al_2O_3$ catalyst often used in WGS reaction was studied by Gines et al in an attempt to compare their calculated results with experimental results in order to predict reaction rates.[21] There was a good agreement between both sets of data when they assumed that both the CO_2 dissociation and the water formation determined the overall reaction rate.

Fujita et al.[23] studied the RWGS reaction mechanism over Cu/ZnO_2. They both suggested that the mechanism proceeds by a surface oxidation of Cu to CuO. H_2 could then reduce CuO to metallic Cu forming H_2O. Campbell et al. also postulated the formation of formate species as a major intermediate.

Chen et al.[24] studied the kinetics of metallic Cu over Al_2O_3 and SiO_2. They also suggested the impact of formate species. They discuss that formats are intermediate

species caused by the association of adsorbed hydrogen atoms with CO_2. In addition, they showed the presence of Cu_2O formed when oxygen atoms react with Cu.

Issues with Cu arise when operating temperatures increase consequently reducing its catalytic activity. Iron was among the first Cu dopants successfully used in the RWGS reaction. The reasoning behind tilizing Fe containing catalysts is taken from their increased thermal stability as shown previously and its good activity towards the WGS reaction.[25] In addition, Fe has a much higher melting point (1535 ℃) than Cu (1083 ℃) making it a good candidate for high temperature reactions.[26] By the addition of Fe as thermal stabilizer, the sintering of Cu particles can be effectively resisted. Chen et al[24] also have successfully synthesized atomic layer Cu/SiO_2 catalysts by which effectively improved catalysts' thermal stability, claiming that the catalyst had different characterization in contrast to standard Cu. What happens in this case is that the Cu particles were prevented from contacting each other. Additionally, they mention that the deposition method provides high catalytic activity for the transformation of CO_2 to CO. This is because sintering was prevented causing no loss in copper surface area.

2.3.2. Ni based catalyst for RWGS reaction

Nickel is another transition metal with good hydrogenation behavior. Its stability at high temperatures is similar to that of Fe with a melting point of 1455 ℃.[26] However Ni is known for its capability to further hydrogenate CO to CH_4, making it a lesser candidate for RWGS reaction.[27] Hydrogenating CO is an undesired step because it inhibits the

application of the FT synthesis which utilizes a syngas mixture to make long chain hydrocarbons or alcohols.

Ni remains a candidate as a catalyst for the RWGS reaction despite its high CH_4 selectivity. This is in large part caused by the high operating temperature used in RWGS reaction. According to Gibbs equilibrium calculations, the CO methanation reaction is strongly favorable at lower temperatures (below 350 ℃).[21] At high operating temperature the methanation reaction is somewhat less favorable which accounts for the use of Ni as a possible catalyst for the RWGS reaction.

Wang et al performed high temperature RWGS experiments using Ni/CeO_2 in order to examine the preparation method and the metal loading effect on the RWGS reaction. They operated at high temperatures (400-750 ℃) and low reactant flow rates (50 mL/min) fed stoichiometrically according to the RWGS reaction.[28] In their work, they found that both the preparation method and the metal loading influenced the results for the RWGS reaction. First, they noticed that the high dispersion of Ni particles formed deficiencies within ceria's crystal lattice creating oxygen vacancies which increased conversion. They also found that 2 wt% loading had the best conversion amongst a range of 0 to 20 wt%. Their catalyst showed high CO formation and some CH_4 yields.

Other groups studied the reaction kinetics on Ni providing in depth analyses of the production of formates on Ni surfaces.[29] The group claims that formate species are a "dead-end spectator molecule." Goguet et al.[30] also suggested that formate species did not actively participate in the reaction. Instead, the reaction pathway would go through a

Eley-Rideal mechanism.

Research on dopants for Ni catalysts has been done in the hopes of increasing CO selectivity. Potassium (K) was amongst the first dopants used with Ni for the RWGS reaction. Campbell et al. looked into adding different weight loadings of K to a Ni/SiO_2 catalyst. The researchers operated at low temperatures (280 ℃) and increased H_2:CO_2 ratios (3.3:1).[31] They noticed an increase in the CO turnover number and a decrease in the CH_4 turnover number with loadings of up to 0.81 wt% K. Their work showed that doping Ni with K can increase CO selectivity.

2.3.3. Pt based catalyst

Precious metals are traditional active heterogeneous catalysts in RWGS reaction due to precious metals are highly active for H_2 dissociation.[32] Researchers have been able to successfully synthesize Pt nanoparticles of specific size and deposit them on varying supports. Pt nanoparticles have been researched for other reactions and have proven to be efficient at relatively small loadings (1 wt% metal, 99 wt% support).[33]

Supported metallic Pt in the micron scale has been tested for the WGS reaction showing promising results. Among these, Pt/ZeO_2, Pt/Fe_2O_3, Pt/CeO_2 and Pt/TiO_2 have all shown considerable yields within the 250-400 ℃ temperature range.[21] These supported catalysts are compared in Table 1 which demonstrates the activation energy and the catalytic activity. Pt/TiO_2 demonstrates the best catalytic activity at 300 ℃ and Pt/Fe_2O_3 shows the worst.

Table 1. Apparent activation energies and catalytic activities (at 300 ℃) of Pt over supported reducible oxides.[21]

Catalyst	Ea (kJ/mol)	Activity (mmol/kg cats)
2% Pt/CeO2	65	15
1.5% Pt/ZrO2	58	20
1.9% Pt/TiO2	23	39
1.5% Pt/FeO3	44	6

In the past 10 years, Pt nanoparticles have been tested for the RWGS reaction. These are typically deposited on reducible supports like TiO_2 and CeO_2 with positive results. The size of the supported Pt particles ranges from 1 nm to 400 nm depending on the researchers conducting the experiments.

Kim et al tested Pt/TiO_2 at different H_2/CO_2 feed ratios in a temperature range of 300 to 600 ℃, with an attempt to modify the reaction conditions in order to form valuable hydrocarbons directly.[34] They used H_2/CO_2 feed ratios of 1:1, 2:1 and 3:1. They were able to shift the equilibrium slightly away from the methanation- which is formed by hydrogenation of CO, by lowering the operating pressure and reducing the H_2/CO_2 ratio. They used a space velocity (SV) of 12000 h^{-1}, 500 mg of catalyst and 1 wt% loading, Pt nanoparticles had an average size of 22 nm. They achieved near equilibrium conversion for their temperature range with no CH_4 production. They also observed an increase in conversion with an increase in H_2:CO_2 feed ratio. However, CH_4 was observed when the ratio was increased to 2. They also observed limited to no deactivation for a period of 72 hours.

The same researchers compared the support's reducibility using Pt nanoparticles.[4] They compared the use of titania (TiO_2) as a reducible support with gamma-alumina (γ-Al_2O_3) using 500 mg of catalyst. They observed a considerable increase in CO_2 conversion when using Pt/TiO_2. They suggest that the support's reducibility is the main cause of their observation.

Goguet et al worked with Pt/CeO_2 studying catalytic deactivation as well as spectrokinetic investigation for the RWGS reaction.[30] In their work, they observed that CO is the main cause of low temperature deactivation. In addition, high H_2/CO_2 ratios combined with extensive catalytic testing can cause an accumulation of coke on the catalytic surface. Their spectrokinetic research concluded that formats are most entirely spectator species in the formation of CO. They also found that Pt bound carbonyls are not a major reaction route. Instead, they concluded that support surface carbonyls are the main reaction intermediate. Figure 3 demonstrates their interpretation of their intermediates formed over Pt/CeO_2 catalysts. These kinetic tests were performed at low temperatures (225 ℃) and high H_2/CO_2 ratios.

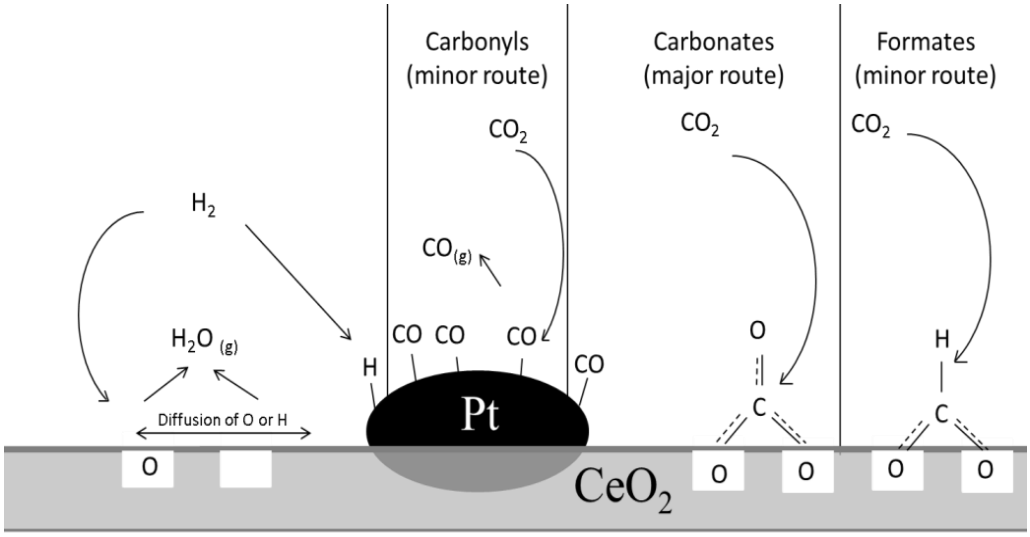

Figure 3. Model for the reaction mechanism of the RWGS reaction over Pt/CeO_2.[30]

However, precious metal has low abundance which is not suitable for large-scale industrial processes. Therefore, Pt-like materials, as alternative catalysts, which are composed of cheap and widely distributed elements, have attracted extensive attention.

2.4. Molybdenum carbide catalysts

Molybdenum is an inexpensive and widely-distributed element, it could form various compounds with the combination of carbide and nitride, from the open literature combined materials will exhibit outstanding catalytic performance.[35] Among them, molybdenum carbide is an excellent choice and has been found superior active for a range of chemical reactions, including CO hydrogenation, methane reforming, isomerization and water gas shift reaction.

Molybdenum carbides have been regarded as the most favorable alternative catalysts to replace precious metals, due to their analogical electronic properties to Pt.[7]

Molybdenum carbides displayed excellent surface catalytic properties resulted from their Pt-liked d-state density, lead to their outstanding catalytic performance and other superior properties in thermal stability, mechanical hardness, superconductivity.[36]

In the particular case of hydrogenation reactions, molybdenum carbide (Mo_2C) has been studied for over 40 years for its potential as a hydrogenating catalyst. Since Levy et al. reported the Pt-like behavior of tungsten carbide.[8] As a catalyst for CO_2 to CO conversion, Chen et al reported that Molybdenum carbide catalyst even outperform monometallic Pt, Pd and Pt-Co, Pd-Co bimetallic catalysts. Thus Molybdenum carbide as a promising candidate for CO_2 conversion to CO still deserves further investigation.

This section is dedicated to highlighting the most pertinent advances in catalysis relevant to molybdenum carbide catalysts, including the crystal structure of molybdenum carbide catalysts, synthesis methodologies, nanowire materials, and possible mechanism.

2.4.1. Molybdenum carbides crystallographic structure

Transition metal carbides usually adopt simple crystallographic structures: face centered cubic, hexagonal closed packed and simple hexagonal; with the carbon atoms occupying the interstitial sites between metal atoms (Figure 4).[37] The crystal structure adopted depends on two factors, the first one geometrical, which states that the structure is formed when the ratio of atomic radii between non-metal to metal is between 0.41 and 0.59 (Hagg's rule),[38] the second one, electronic, states that bonding between s-p orbitals from the non-metal and the s-p-d orbitals from the metal atoms is due to overlap and the

bond strength depends on the number of d electrons in the metal.

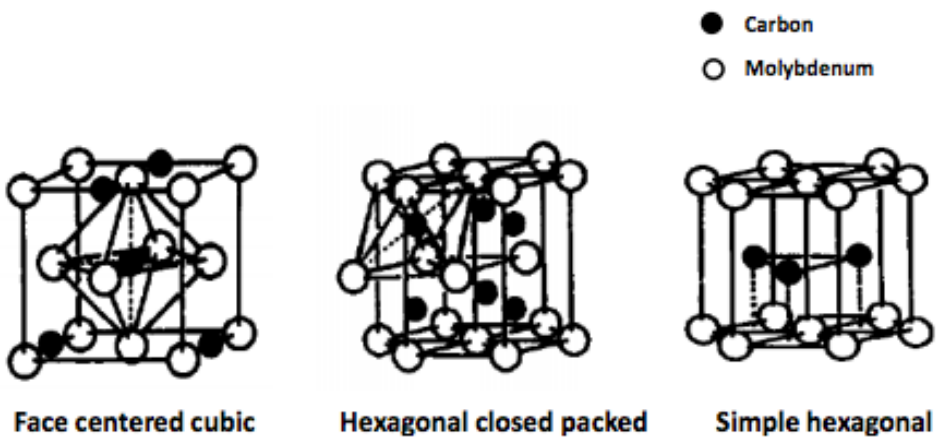

Figure 4. Common crystallographic structures of transition metal carbides. [37b]

α-MoC_{1-x} and β-Mo_2C are traditional phases,[12] α-MoC_{1-x} has face center cubic structure while β-Mo_2C has a hexagonal close-packed structure. α-MoC_{1-x} is a metastable phase while β-Mo_2C is thermodynamically stable.

In Brian M. Leonard's work,[39] α, β, γ and η phase nanowires has been successfully synthesized (Figure 5). The catalytic performance was compared in Hydrogen evolution reaction (HER), the β-Mo_2C exhibited the highest HER activity, γ-MoC shows similar activity to β-Mo_2C, while α-MoC_{1-x} and η-MoC exhibit the lowest HER activity.

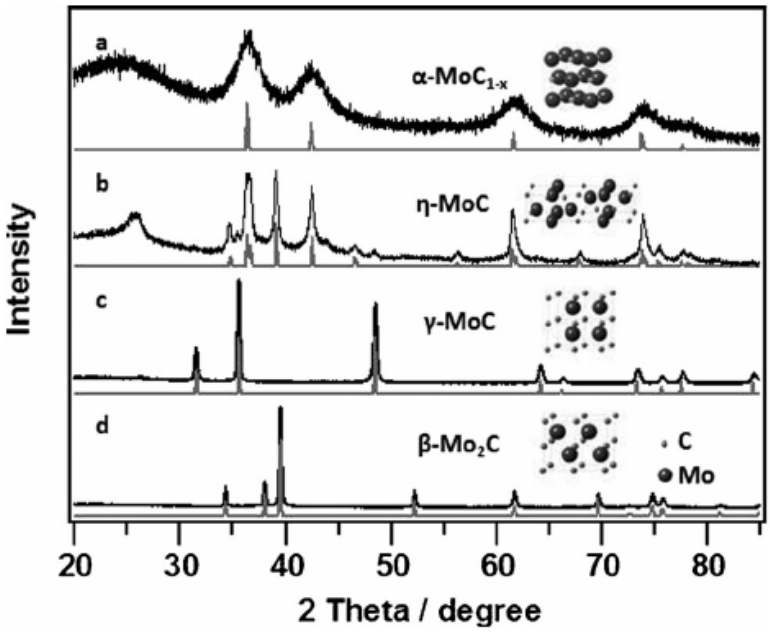

Figure 5. X-ray diffraction (XRD) patterns of a) α-MoC_{1-x} (JCPDS 01-089-2868), b) η-MoC (JCPDS 01-089-4305), c) γ-MoC (JCPDS 00-045-1015), and d) β-Mo_2C (JCPDS 00-011-0608). The insets show the corresponding crystal structures.[39]

From the open literature, results showed that molybdenum carbide with β phase is usually the most active in variety of reactions,[40] while the activity of α phase is far less than β phase. In shen et al.'s work,[41] the high activity of β phase was attributing to the more coordinatively unsaturated Mo sites on the surface.

The crystal structure not only affects the catalytic activity but also the reaction product distribution. In Xu's work,[42] α-MoC_{1-x} and β-Mo_2C were synthesized for CO_2 hydrogenation reaction, results showed that α-MoC_{1-x} and β-MoC_y both active as catalysts for CO_2 hydrogenation. But the overall activity towards CO, CH_4, and CH_3OH production is strongly affected by the crystal structure. β-Mo_2C is more active than

α-MoC_{1-x} for the conversion of CO_2 and mainly produce methane and CO as reaction products. On the other hand, α-MoC_{1-x} is less active but more selective for methanol production.

2.4.2. Molybdenum carbide synthesis methodologies

Conventional preparation techniques involve the reaction of the metals, metal hydrides, or metal oxides with C in reducing atmosphere at very high temperature (more than 1500K). With low Sg and impurity, this synthesis method cannot be used for the production of efficient catalysts.[43]

TPRe method is also a popular method for preparation of Mo_2C, the metallic powder of the transition metal or its oxide is reacted with a carbon source under a stepwise temperature increase protocol.[44] Usually, a gaseous mixture of hydrocarbons is enough to entirely carburize the respective precursor under the temperature programmed method. The disadvantage of this method is the surfaces easily contaminated in surface carbon and the synthesis process requires very critical heating procedure and gas atmosphere.

Chemical vapor deposition involves the use of metallic halide vapors (mostly chlorides) that are reacted with gaseous hydrocarbons and the carbide formed is deposited on a heated filament.[45] Typically, the reaction is carried out at 600 ^{o}C. The purity of the species obtained is incredibly high as well as the control over the reaction.

Recently, a novel organic-inorganic hybrid method for synthesis molybdenum carbide nanowires is reported,[46] MoO_x/amine was employed as nanocomposite precursor,

with such organic-inorganic precursor, during carburization, quasi-homogeneous reactions could happen uniformly. Compared with TPRe method, organic-inorganic method avoids the interface reactions. The preparation of Mo_2C nanowires were through easily calcining MoO_x /amine nanowires in the Ar atmosphere. The as-obtained large surface area Mo_2C porous nanowires will be composed of small nanoparticles, which lead to their superior activity in many catalytic reactions.

2.4.3. Synthesis of molybdenum carbide nanowires

The formation of $Mo_3O_{10}(C_6H_5NH_3)_2\ 2H_2O$ precursor was through a self-assembly method to attach protonated aniline to trimolybdate anions, anisotropic growth of anilinium trimolybdate forms 1D nano-rods at 50 ^oC.

The mechanism of the formation of Mo_xC_y is that amine molecules act as reducing compound and resource of C during the carburization process. Molybdenum oxide is reduced by the C and N atom in the precursor during carburization, finally form the molybdenum carbide.

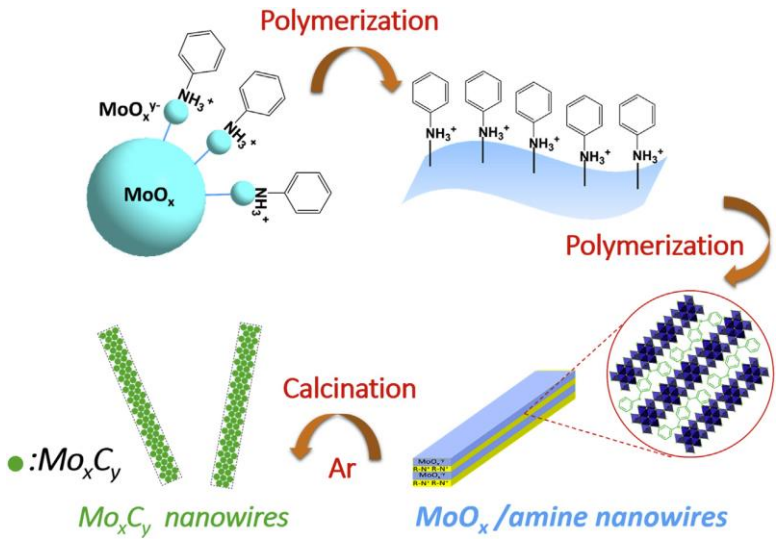

Scheme 1. Molybdenum carbide nanowire formation mechanism[47]

2.5. Mechanism of RWGS reaction on molybdenum carbide catalyst

In Chen's work[9] proposed a mechanism of RWGS reaction on molybdenum carbide catalyst. CO_2 easily dissociated on Mo_2C catalyst with O atom on the catalyst, the molybdenum carbide oxide then can be reduced by H_2. They use in situ-XPS technique confirmed oxycarbides species during reaction. The In situ-XPS measurements on Mo_2C do not show evidence supporting the presence of carbonate (CO_3), carboxyl (CO_2-) and formate (HCOO) as the reaction intermediates.

In the work of Xu et al, they discovered on β-Mo_2C, carbon dioxide probably undergoes sequential decomposition.[42] These trends are consistent with the results of DFT calculations of CO_2 adsorption on a β-Mo_2C (001). The calculations show that the cleavage of CO_2 C-O bond and formed CO and O on the surface. While the cleavage of the second C-O bond can only happen at very high temperature. In principle, a Mo-rich

surface makes Mo-C bonds from adsorbed CO_2 while a C-rich material may not, on the C-rich α-MoC1-x product, methane is always a minority product, DFT calculations examining the adsorption of CO_2 on MoC(001) surfaces show only chemisorption of the molecule without cleavage of the C-O bonds, on these C-rich carbides, cleavage of the first C-O bond in CO_2 occur only through hydrogenation and formation of a HOCO intermediate, which eventually decomposes into CO that upon subsequent hydrogenation yields methanol. In the case of α-MoC_{1-x}, the catalyst does not have exactly a metal/carbon ratio of one and, thus, some of the adsorbed molecules still undergo a CO2→CO→C→CH_4 transformation, but the main chemistry is clearly that of C-rich carbide yielding mostly CO and CH_3OH as products of the hydrogenation of CO_2.

Jose et al. studied the kinetics of the WGS reaction.[48] They found that the Oxygen covered Mo-Mo_2C (001) surface has the lowest activity due to O-Mo-Mo_2C surface cannot effectively adsorb CO or dissociate H_2O. However, small amount of O on the C-Mo_2C promote the WGS reaction, due to the formation of Mo oxycarbide, in this wany enhanced the catalytic performance.

3. Experimental section

3.1. Experimental approach

This experimental approach in this thesis consists of three main parts, preparation of catalysts, catalyst characterization and kinetic measurements for each catalyst. Here under, each moment is described in more detail and some background information of characterization method is given as well.

3.2. Catalyst preparation

3.2.1. MoO_x/aniline Precursor preparation

Nanowires molybdenum carbide was prepared through an organic–inorganic hybrid method under 5% H_2/Ar atmosphere. MoO_x/aniline hybrid precursors ($Mo_3O_{10}(C_6H_5NH_3)_2 \cdot 2H_2O$) was prepared as follows: In detail, 2.48 g of $(NH_4)_6Mo_7O_{24} \cdot 4H_2O$ and 3.34 g of aniline were dissolved in 120 ml of DI-water. Then 1.0 M HCL was dropwise added with magnetic stirring until precipitate formed. Then it was heated at 50 ^oC for 6h, afterwards the product was filtered and washed with ethanol for several times, and then dried at 80 ^oC overnight.

3.2.2. Molybdenum carbide nanowires preparation

MoO_x/aniline precursor was carburized in a tube furnace in 5%H_2/Ar atmosphere.

Air in the quartz tube was purged out by 5%H_2/Ar at room temperature for 4h, Then heated to specific carburization temperature with a ramping temperature rate of 2 ^{o}C /min，and hold at final temperature for 3.5 h. Before exposure to air, the sample was quenched to room temperature and naturally cooled down before taken out.

3.3. Characterization

Crystalline structure of the catalyst was determined by X-ray diffraction (XRD). Characterization was conducted with a Bruker diffractometer employing Cu Ka radiation (40 kV and 44 mA). Single-point Brunaeur–Emmett–Teller (BET) surface area was measured through nitrogen adsorption at liquid-nitrogen temperature(77 K) using an ASAP-2000 Micromeritics instrument. Transmission electron microscopy (TEM) images were taken using a JEOL-2011 microscope at 200 kV. In-situ X-ray photoelectron spectroscopy (In-situ XPS) experiments were carried out with aPHI-5300 X photoelectron spectrometry employing a Al-Ka X-ray source, The binding energy of the samples was corrected with the energy of C1s (284.6 eV) as the reference. DRIFTS analysis was performed on a Digilab Excalibur FTIR spectrometer. The sample was firstly reduced conditioned at 400℃ in H_2. Then, the sample was cooled to room temperature, the CO_2 and CO were separately introduced in to the DRIFTS cell at room temperature.

3.4. Reaction experiments

The catalytic performance for each catalyst was analyzed in a continuous gas flow in a fixed bed reactor. The reactor contains a coated monolith catalyst surrounded by two uncoated monoliths, placed close to the outlet. 50 mg catalyst was packed and the monoliths were wrapped in a thin layer of quartz wool to prevent bypassing of gas. One thermocouple was placed in the middle of the catalyst and another one in the middle of the first monolith. The tests started with 30 min of treatment in H_2 at 500℃. Each catalysts was investigated in the temperature range of 200-500 ^{o}C with an almost 9. A gas mixture of 75 % He/5 % CO_2 /20 % H_2 at a total flow rate of 200 ml/min under atmospheric pressure. The effluent gas from the micro-reactor was analyzed by an online gas chromatography with Flame ionization detector (FID). The CO_2 conversion was based on the CO formation.

4. Results

4.1. Pure phase study

This pure phase study in this thesis consists of three main parts, structural characterization, catalyst performance and surface property study for each catalyst. Herein, each section is described in more detail and some background information of characterization method is given as well.

4.1.1. Structural characterization

Figure 6 shows XRD pattern and TEM images of the as prepared multiple phases of molybdenum carbide nanowire. The β-Mo_2C was prepared by carburizing the $Mo_3O_{10}(C_6H_5NH_3)_2 \cdot 2H_2O$ precursor at 750 °C (denoted β-750) for 3.5 h under 5%H_2/Ar atmosphere. It exhibited characteristic diffraction lines of the β phase (JCPDS#35-0787) and had a width of about 60 nm and lengths of 0.5-7 μm. β-Mo_2C had pores of about 2.2 nm on the surface and a surface area of 46 m^2/g, which is comparable with the result from literature.

While Figure 6a α-MoC_{1-x} was synthesized at 700 °C for 3.5 h under 5%H_2/Ar atmosphere (denoted α-700). The product showed diffraction lines of α-MoC_{1-x}, the BET surface area of α-MoC_{1-x} synthesized at 700℃ was 161 m^2/g. Figure 6d α-MoC_{1-x} was synthesized by carburizing the $Mo_3O_{10}(C_6H_5NH_3)_2 \cdot 2H_2O$ precursor at 720 °C for 3.5 h under 5%H_2/Ar atmosphere (denoted α-720). The diffraction peaks of α-720 were similar

with α- 700. The BET surface area of α-720 was 216 m^2/g, The lattice of α-720 (~0.238nm) was similar with α-700 (~0.239nm).

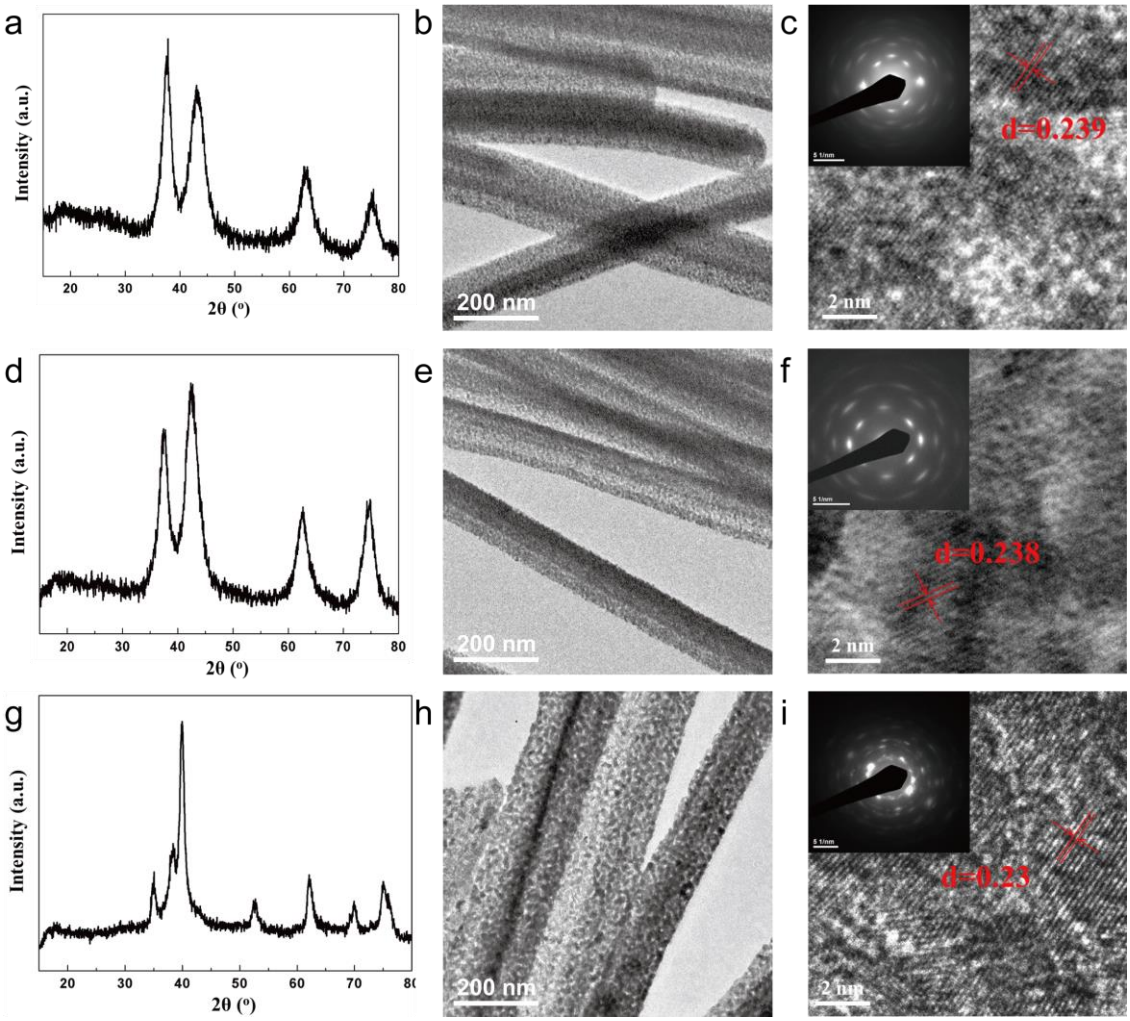

Figure 6. XRD patterns, TEM images and HRTEM images of α 1 (a-c) α 2 (d-f) β (g-i) and (inset of c, f and i) SAED patterns of the corresponding nanowires.

4.1.2. Catalytic performance

Catalytic performances of molybdenum carbide (α, β phase and commercial) catalyst for the CO_2 reduction to CO were evaluated in details in a temperature range of 200 °C to 450 °C with a GHSV 24000h^{-1}. The CO_2 conversion profiles of molybdenum

carbide catalyst are presented in Figure 7. The CO yield increases with temperature as expected by thermodynamics. From Figure 7a ,it is found that the catalytic performances of the α-700 was very poor, which is comparable with commercial Mo_2C, although α-700 has relatively larger surface area, the intrinsic activity of each active site on the α-700 was very low, the activity of α-720 were higher than that of β-750.

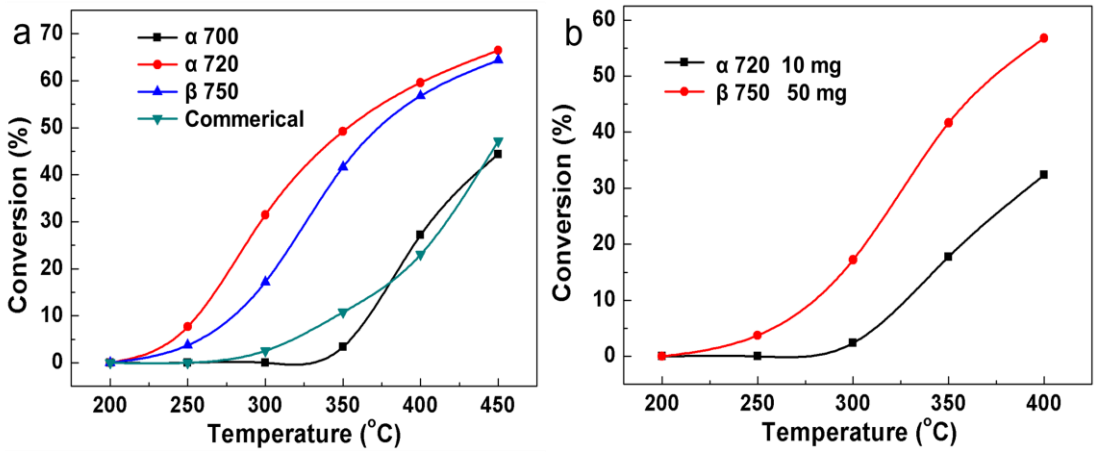

Figure 7. Apparent activity test (a), surface area normalized activity (b).

From the BET results it is found that the surface area of α-720 is very high, 4 times higher than β-750, it is anticipated that the intrinsic activity of β-750 is higher than α-720. The suface area normalized conversion in Figure 5b showed the roughly comparison of α-720 and β-750. It shows the intrinsic activity of β-750 is higher than α-720. For all 3 catalyst, CO is the main product in the out let gas, together with a small amount of CH_4, indicate the superior selectivity of molybdenum carbide catalyst, the 50 h stability test at 600 °C (Figure 8) shows molybdenum carbide is a very durable catalyst for CO_2 to CO reaction.

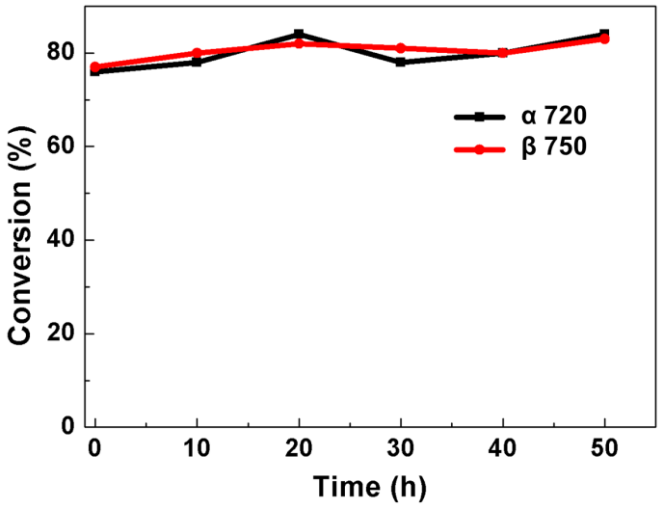

Figure 8. Stability test: conversion vs time.

4.1.3. Surface property

The In-situ XPS measurement is applied to investigate the surface properties and reducibility of the molybdenum carbide catalysts upon reduction, and the corresponding results of Mo3d and C1s of each sample are given in Figure 9 and 10.

From Figure 9, Mo^{6+} is characteristic of oxidized phases, resulting from the ambient oxidation in passivation step. The Mo^{6+} content of α-720 is significantly lower than α-700 and β-750, indicating lower amount of MoO_3 structure exist in the sample. Conversely the α-720 is rich in lower valence state of Mo^{5+}, Mo^{4+}, Mo^{2+}, result from the past demonstrated that lower valence state Mo^{5+}, Mo^{4+} and Mo^{2+} also regarded as unsaturated Mo metal centers which will alter the catalytic performance. Upon reduction, for all 3 samples, the amount of Mo^{6+} species all significantly reduced, large amount of Mo^{6+} convert to Mo^{4+} and Mo^{2+} species, which can be found even without fitting. β-750 catalyst is the most easily to be reduced among the 3 catalysts. While α-700 is the most

inert sample considering the reducibility. From the In-situ XPS results it can be anticipated that the superior intrinsic activity of β-750 owing to its high reducibility ability, although the surface area only 1/4 of α phase catalyst. The assignment area of different valence state and surface atom content are listed in table 2 and 3.

For each C1s spectrum, the peak at about 284.6 eV is assigned to the C-C bonds, before reduction, large amount of surface carbon on the molybdenum carbide catalysts. Also C=O species and low amount of C-Mo species existed on the surface. Upon reduction, the amount of C-C species significantly reduced, and large amount of Mo-C species generated on the catalyst surface. C=O species disappeared after H_2 reduction. For α-700, the amount of Mo-C generated on the surface is far less than β-750, which may account for its low intrinsic activity. It can be anticipated that Mo-C species are the active species on the catalyst, which served as active centers for CO_2 adsorption and dissociation on the molybdenum carbide catalyst.

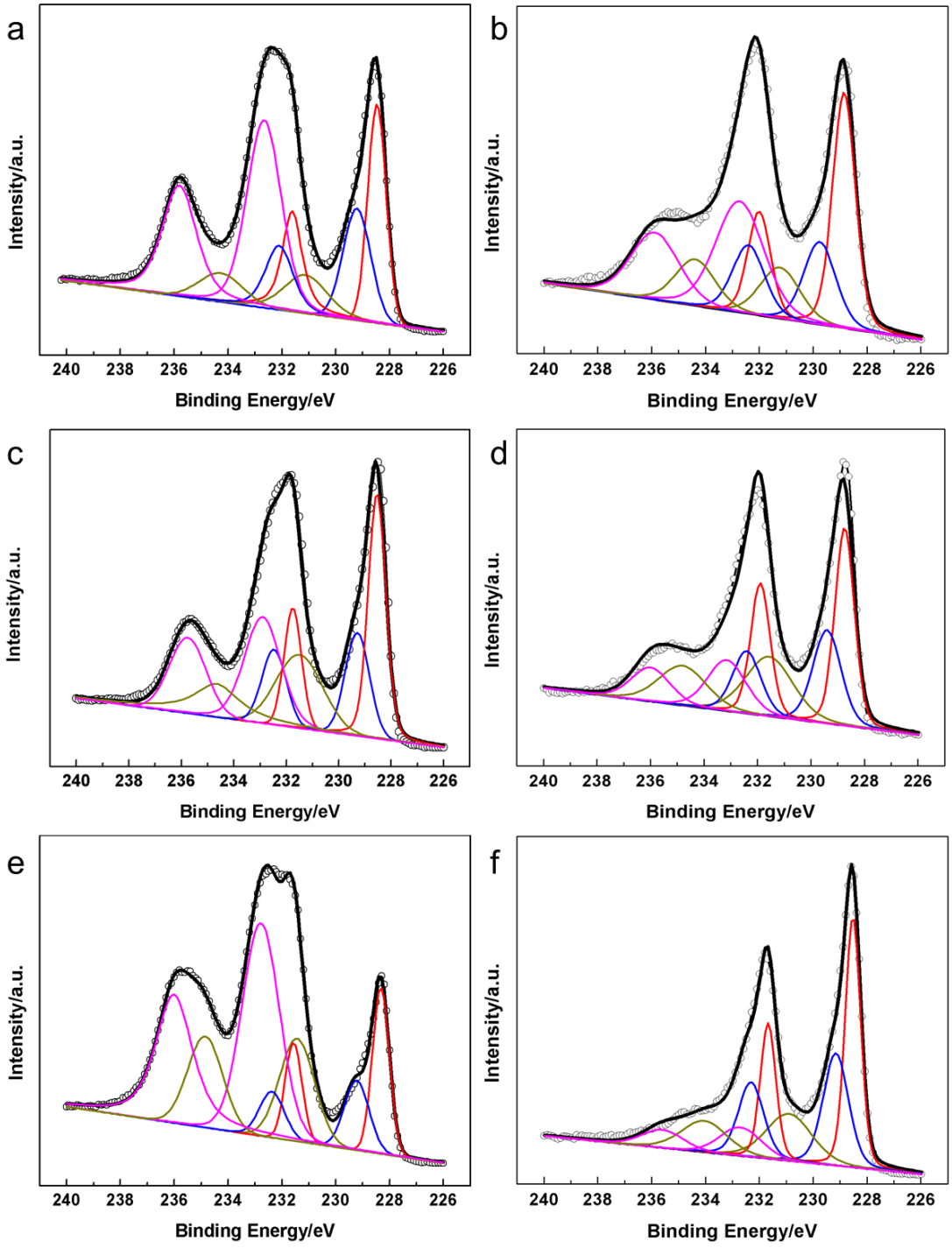

Figure 9. XPS Mo3d spectra and the fitting peaks of α 1 (a and b) α 2 (c and d) β (e and f).

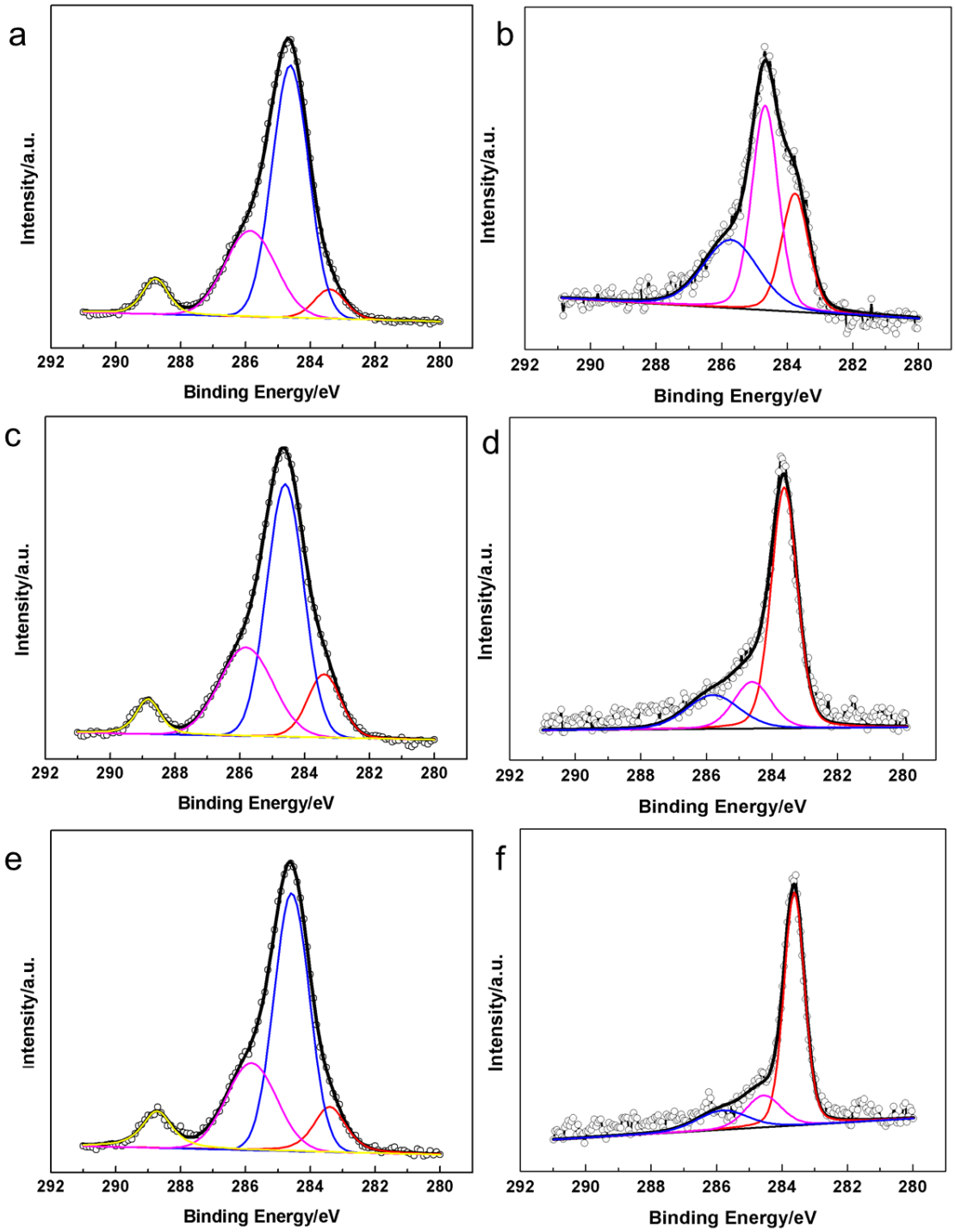

Figure 10. XPS C1s spectra and the fitting peaks of α 1 (a and b) α 2 (c and d) β (e and f).

Table 2. Quantitative analysis of Mo_3d signals for MoC catalysts (r for reduction)

Catalyst	Assignment	B.E. (eV)	Area (%)
α-700	Mo^{6+}	232.10	43.9
	Mo^{5+}	231.62	11.7
	Mo^{4+}	229.21	19.3
	Mo^{2+}	228.47	25.1
α-700-r	Mo^{6+}	232.73	34.2
	Mo^{5+}	231.23	15.6
	Mo^{4+}	229.75	19.2
	Mo^{2+}	228.86	31.0
α-720	Mo^{6+}	232.47	29
	Mo^{5+}	231.75	24
	Mo^{4+}	229.29	18.2
	Mo^{2+}	228.54	28.8
α-720-r	Mo^{6+}	233.15	17.4
	Mo^{5+}	231.56	25.2
	Mo^{4+}	229.40	23.2
	Mo^{2+}	228.74	34.2
β-750	Mo^{6+}	232.37	50.5
	Mo^{5+}	231.57	23.8
	Mo^{4+}	229.22	10
	Mo^{2+}	228.33	15.7
β-750-r	Mo^{6+}	232.70	11.5
	Mo^{5+}	230.90	22.2
	Mo^{4+}	229.16	29.1
	Mo^{2+}	228.53	37.2

Table 3. Quantitative analysis of C1s signals for MoC catalysts (r for reduction)

Catalyst	Assignment	B.E. (eV)	Area (%)
α-700	Mo-C	283.4	6
	C-C	284.61	59.1
	C-O	285.85	28
	C=O	288.78	6.9
α-700-r	Mo-C	283.763	25.8
	C-C	284.673	43.6
	C-O	285.72	30.6
α-720	Mo-C	283.4	12.8
	C-C	284.60	53.8
	C-O	285.80	27.4
	C=O	288.83	6
α-720-r	Mo-C	283.62	64.2
	C-C	284.6	17.6
	C-O	285.8	18.2
β-750	Mo-C	283.4	10.8
	C-C	284.57	54.3
	C-O	285.81	26
	C=O	288.72	8.9
β-750-r	Mo-C	283.62	69.6
	C-C	284.57	16.3
	C-O	285.82	14.1

Table 4. BET area and surface compositions of MoC

Catalyst	S_{BET} (m^2 g^{-1})	Surface atom content (mol%)		
		X_{Mo}	X_C	X_O
α-700	161	11.1	63.4	25.5
α-720	216	15.3	56.8	27.9
β-750	46	16.2	43.8	40.0

4.2. Mix phase study

4.2.1. Phase transformation

In order to have a further understanding of the relationship between the crystal structures with the catalyst performance, we studied the phase transformation from pure α phase to pure β phase. 3 key mix phases between α and β phase were captured, denoted as α dominant， half mix, β dominant, respectively. The catalytic performance of molybdenum carbide with mix phases also tested for comparison.

From the phase transformation and the XRD pattern of 3 key mix phases (Figure 11), together with pure α and β phase. If set α phase status as a start point, during carburization, the peak at 39.8 ^oC emerges primarily, which is the characteristic peak of β phase Mo_2C structure emerged. Then the 39.8 ^oC peak intensity become higher while α phase characteristic peak 42.8 ^oC become weaker, the 34.8 ^oC peak secondly generated, eventually the β Mo_2C peak all significantly generated and with only small amount of α phase remaining.

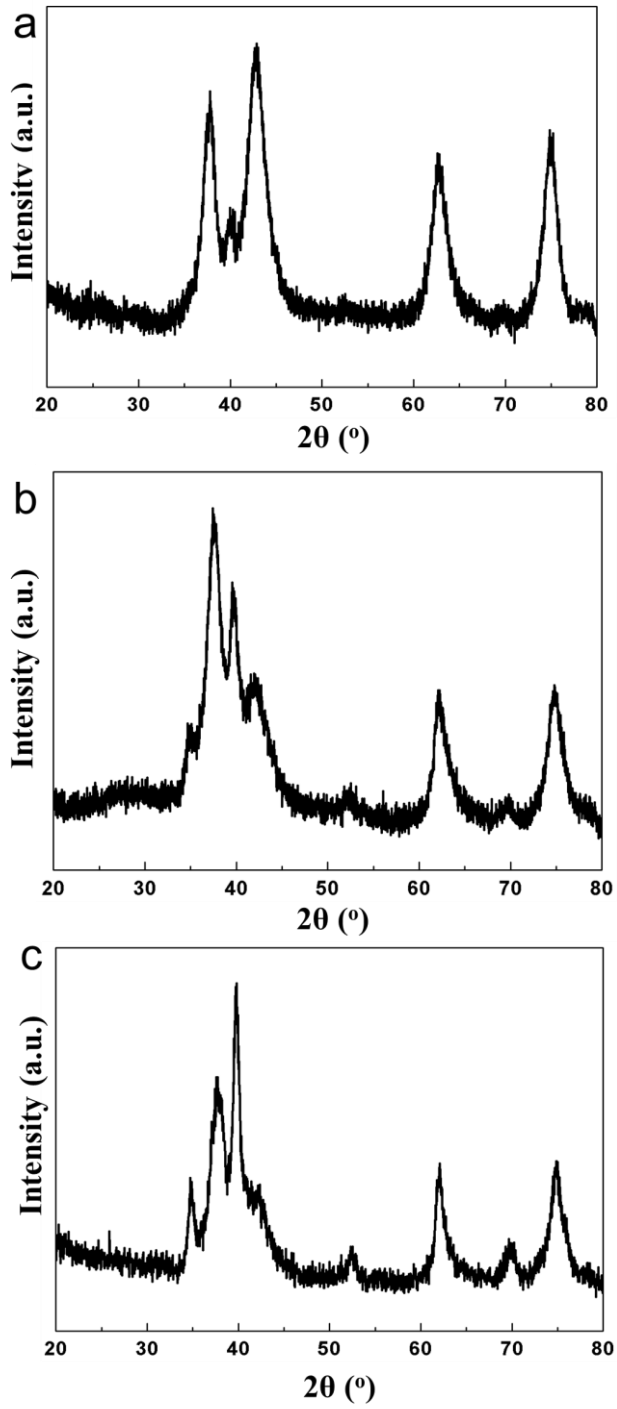

Figure 11. XRD patterns of α dominant (a), half mix (b), and β dominant (c).

4.2.2. Catalytic performance

The activity results showed that mix phase activity all in between of the pure α and β phase, the BET surface area of α dominant, half mix, β dominant were 117, 75, 50 m^2/g respectively. During carburization process, the surface area reduced, together with the reaction sites become more active. (Figure 12).

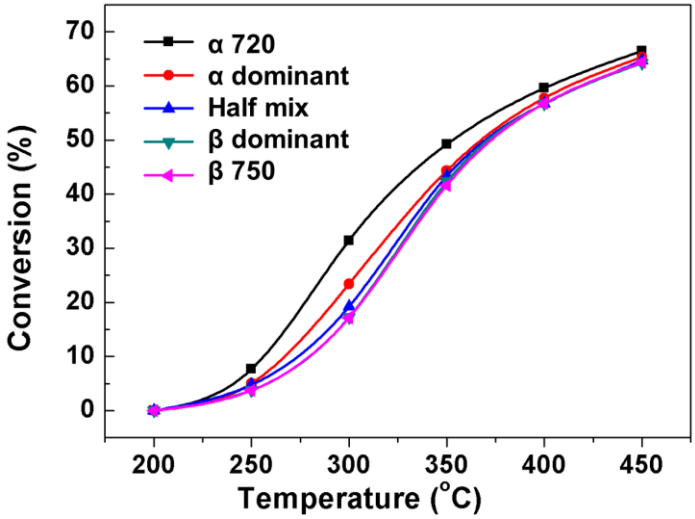

Figure 12. Apparent activity of mix phase molybdenum carbide catalysts.

4.3. DRIFTS study on CO_2 and CO adsorption

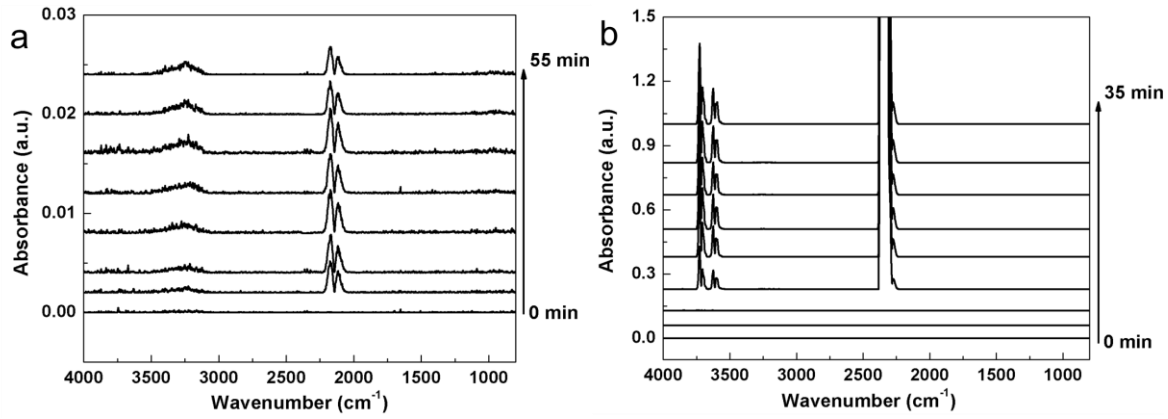

Figure 13. DRIFTS spectrum of CO adsorption (a) and CO_2 adsorption (b).

Diffuse Reflectance Infrared Fourier Transform Spectroscopy (DRIFTS) was used to test the CO_2 and CO adsorption. The CO adsorption is very weak compared with CO_2 adsorption on reduced molybdenum carbide catalyst, which account for molybdenum carbide catalyst's high selectivity behavior.

5. Discussion

The main goal of the thesis was to investigate the characterize properties of molybdenum carbide catalysts with difference crystal phases, synthesis durable molybdenum carbide catalysts with enhanced catalytic performance, and gain further understanding of RWGS reaction mechanism on molybdenum carbide catalysts.

Crystal-phase control and shape control synthesis of molybdenum carbide has become significant approaches to improve molybdenum catalyst's performance, cause the catalytic properties of molybdenum carbide catalyst are closely linked with their crystal structure, size and shape.

The physical characterization of molybdenum carbide catalysts produced several important results. Generally α phase catalyst has superior surface area compared with β phase catalyst. The conversion of α-MoC_{1-x} into active α phase was achieved by slightly elevates the carburization temperature from 700 ^{o}C to 720 ^{o}C. In-situ XPS result showed the transformation of α-MoC_{1-x} into active α phase owing to active α phase catalyst's enhanced reducibility and generation of large amount of Mo-C active species.

From the In-situ XPS results it can be anticipated that the superior intrinsic activity of β-750 owing to its high reducibility ability, although the surface area only 1/4 of α phase catalyst. It can be anticipated that Mo-C species are the active species on the catalyst, which served as active centers for CO_2 adsorption and dissociation on the molybdenum carbide catalyst.

DRIFTS was used to test the CO_2 and CO adsorption. The CO adsorption is very weak compared with CO_2 adsorption on reduced molybdenum carbide catalyst, which account for molybdenum carbide catalyst's high selectivity behavior.

In Chen's work[9] proposed a mechanism of RWGS reaction on molybdenum carbide catalyst. CO_2 easily dissociated on Mo_2C catalyst with O atom on the catalyst, the molybdenum carbide oxide then can be reduced by H_2. They use In situ-XPS technique confirmed oxycarbides species during reaction. In our work we also confirm the existence of Mo-C species upon H_2 reduction and Mo-C species serve as the active species on molybdenum carbide catalyst.

In Ma et al's work,[47] XPS analysis indicated that the deactivation of molybdenum carbide in SRM reaction is due to surface oxidation. We also synthesized molybdenum carbide catalyst with oxide species, the activity about 10% lower, indicating that in order to improve the catalytic activity, the amount of molybdenum oxide must be reduce for a better catalytic performance.

6. Conclusion & Future outlook

In this research, the most prominent results in this study is the discovery of the reducibility difference of different crystal phases, Mo-C species serve as the active species on molybdenum carbide catalyst. In-situ XPS result showed the transformation of α-MoC_{1-x} into active α phase owing to active α phase catalyst's enhanced reducibility and generation of large amount of Mo-C active species. With In-situ XPS technique, we discovered the reducibility of β-Mo_2C was significantly higher than α-MoC_{1-x}, which corresponded to β-Mo_2C catalyst high intrinsic activity. We then conclude the reducibility difference, closely linked to crystal structure difference, and strongly affected the catalytic performance. DRIFTS was used to study the adsorption properties of molybdenum carbide nanowires catalyst. We proposed the weak adsorption of CO on molybdenum carbide catalyst account for high selectivity behavior. Molybdenum carbide catalysts also serve as very durable catalysts for RWGS reaction considering the 50 h stability test at 600 ^{o}C. We also synthesized series of mix phase molybdenum carbide nanowires and compared the catalytic performance. During carburization process, the surface area reduced, together with the reaction sites become more active.

Suggestions for future outlook, based on ideas emerged during this thesis, the future works are the investigation of the surface property in detail, the exact amount of Mo, C, O, N need to be tested for a further understanding. Also how the active species participate in the RWGS reaction need to be investigated. In order to gain deeper understanding of

RWGS reaction mechanism, despite of CO_2 adsorption, H adsorptions need to be evaluated for the next step. CO chemisorption needs to be conducted for estimate the amount of active sites on molybdenum carbide catalyst. In our previous work, although we have removed the polymeric carbon and achieved a better catalytic property, the coke on the surface still need to further removed, a proper duration of H_2 treatment will be used for the coke removal. Electron paramagnetic resonance and Auger electron spectroscopy will be used as characterization technique for quantify the coke on the molybdenum carbide surface.

References

1. Zachos, J.; Pagani, M.; Sloan, L.; Thomas, E.; Billups, K., Trends, rhythms, and aberrations in global climate 65 Ma to present. *science* **2001,** *292* (5517), 686-693.
2. Liu, Q.; Wu, L.; Fleischer, I.; Selent, D.; Franke, R.; Jackstell, R.; Beller, M., Development of a ruthenium/phosphite catalyst system for domino hydroformylation-reduction of olefins with carbon dioxide. *Chemistry-A European Journal* **2014,** *20* (23), 6888-6894.
3. Xiong, J.; Dong, X.; Song, Y.; Dong, Y., A high performance Ru–ZrO2/carbon nanotubes–Ni foam composite catalyst for selective CO methanation. *Journal of Power Sources* **2013,** *242*, 132-136.
4. Kim, S. S.; Lee, H. H.; Hong, S. C., A study on the effect of support's reducibility on the reverse water-gas shift reaction over Pt catalysts. *Applied Catalysis A: General* **2012,** *423-424*, 100-107.
5. Mariño, F.; Descorme, C.; Duprez, D., Supported base metal catalysts for the preferential oxidation of carbon monoxide in the presence of excess hydrogen (PROX). *Applied Catalysis B: Environmental* **2005,** *58* (3-4), 175-183.
6. Goguet, A.; Meunier, F. C.; Tibiletti, D.; Breen, J. P.; Burch, R., Spectrokinetic investigation of reverse water-gas-shift reaction intermediates over a Pt/CeO2 catalyst. *Journal of physical chemistry B* **2004,** *108* (52), 20240-20246.
7. Xiao, P.; Yan, Y.; Ge, X.; Liu, Z.; Wang, J.-Y.; Wang, X., Investigation of molybdenum carbide nano-rod as an efficient and durable electrocatalyst for hydrogen evolution in acidic and alkaline media. *Applied Catalysis B: Environmental* **2014,** *154-155*, 232-237.
8. Levy, R. B.; Boudart, M., Platinum-like behavior of tungsten carbide in surface catalysis. *Science* **1973,** *181*, 547-549.
9. Porosoff, M. D.; Yang, X.; Boscoboinik, J. A.; Chen, J. G., Molybdenum carbide as alternative catalysts to precious metals for highly selective reduction of CO_2 to CO. *Angewandte Chemie* **2014,** *53* (26), 6705-6709.
10. Beckman, E. J., Supercritical and near-critical CO_2 in green chemical synthesis and processing. *The Journal of Supercritical Fluids* **2004,** *28* (2-3), 121-191.
11. Ferey, G.; Serre, C.; Devic, T.; Maurin, G.; Jobic, H.; Llewellyn, P. L.; De Weireld, G.; Vimont, A.; Daturi, M.; Chang, J. S., Why hybrid porous solids capture greenhouse gases? *Chemical Society reviews* **2011,** *40* (2), 550-562.
12. Wang, W.; Wang, S.; Ma, X.; Gong, J., Recent advances in catalytic hydrogenation of carbon dioxide. *Chemical Society reviews* **2011,** *40* (7),

3703-3727.
13. B., H.; Suib, S. L., Chapter 3: Synthesis of Useful Compounds from CO_2. *Green Carbon Dioxide: Advances in CO_2 Utilization* **2014**, 51-97.
14. Anpo, M.; Yamashita, H.; Ikeue, K.; Fujii, Y.; Zhang, S. G.; Ichihashi, Y.; Park, D. R.; Suzuki, Y.; Koyano, K.; Tatsumi, T., Photocatalytic reduction of CO2 with H2O on Ti-MCM-41 and Ti-MCM-48 mesoporous zeolite catalysts. *Catalysis Today* **1998,** *44* (1-4), 327-332.
15. Hara, K.; Kudo, A.; Sakata, T., Electrochemical reduction of carbon dioxide under high pressure on various electrodes in an aqueous electrolyte. *Journal of Electroanalytical Chemistry* **1995,** *391* (1-2), 141-147.
16. Drake, B. G.; GonzalezMeler, M. A.; Long, S. P., More efficient plants: A consequence of rising atmospheric CO_2? *Annual Review of Plant Physiology and Plant Molecular Biology* **1997,** *48*, 609-639
17. Olah, G. A.; Goeppert, A.; Prakash, G. K. S., Chemical Recycling of Carbon Dioxide to Methanol and Dimethyl Ether: From Greenhouse Gas to Renewable, Environmentally Carbon Neutral Fuels and Synthetic Hydrocarbons. *The Journal of Organic Chemistry* **2009,** *74*, 487–498.
18. (a) Lee, J. F.; Chern, W. S.; Lee, M. D.; Dong, T. Y., Hydrogenation of Carbon Dioxide on Iron Catalysts Doubly Promoted with Manganese and Potassium. *The Canadian Journal of Chemical Engineering* **2009,** *70*, 511–515; (b) Fujimoto, K.; Shikada, T., Selective synthesis of C2-C5 hydrocarbons from carbon dioxide utilizing a hybrid catalyst composed of a methanol synthesis catalyst and zeolite. *Applied Catalysis* **1987,** *31*, 13–23.
19. M., B., The Basis and Application of Heterogeneous Catalysis. *OXFORD UNIVERSITY PRESS* **1998**.
20. Zeigarnik, A. V.; Callaghan, C.; Datta, R.; Fishtik, I.; Shustorovich, E., Prediction of Comparative Catalytic Activity in the Series of Single Crystalline Surfaces in a Water-Gas Shift Reaction. *Kinetics and Catalysis* **2005,** *46* (4), 509-515.
21. Ratnasamy, C.; Wagner, J. P., Water Gas Shift Catalysis. *Catalysis Reviews* **2009,** *51* (3), 325-440.
22. (a) Tsai, J.; Nicholas, K. M., Rhodium-Catalyzed Hydrogenation of Carbon Dioxide to Formic Acid. *Journal of the American Chemical Society* **1992,** *114*, 5117–5124; (b) Dagle, R. A.; Platon, A.; Palo, D. R.; Datye, A. K.; Vohs, J. M.; Wang, Y., PdZnAl catalysts for the reactions of water-gas-shift, methanol steam reforming, and reverse-water-gas-shift. *Applied Catalysis A: General* **2008,** *342* (1-2), 63-68; (c) Theleritis, D.; Souentie, S.; Siokou, A.; Katsaounis, A.; Vayenas, C. G., Hydrogenation of CO2over Ru/YSZ Electropromoted Catalysts. *ACS Catalysis* **2012,** *2* (5), 770-780.
23. Fujita, S. I.; Usui, M.; Takezawa, N., Mechanism of the reverse water gas shift
reaction over Cu/ZnO catalyst. *Journal of Catalysis* **1992,** *154* (96), 220-225.

24. Chen, C.; Cheng, W.; Lin, S., Study of reverse water gas shift reaction by TPD , TPR and CO2 hydrogenation over potassium-promoted Cu/SiO2 catalyst. *Applied Catalysis A: General* **2003,** *238*, 55-67.
25. Júnior, I. L.; Millet, J. M.; Aouine, M.; Maria, C. R., The role of vanadium on the properties of iron based catalysts for the water gas shift reaction. *Applied Catalysis A: General* **2005,** *283* (1-2), 91-98.
26. Twigg, M. V.; Spencer, M. S., Deactivation of supported copper metal catalysts for hydrogenation reactions. *Applied Catalysis A: General* **2001,** *212* (1-2), 161-174.
27. Schild, C.; Wokaun, A.; Koeppel, R. A.; Baiker, A., CO2 Hydrogenation over Nickel /Zirconia Catalysts from Amorphous Precursors : On the Mechanism of Methane Formation. *The Journal of Physical Chemistry* **1991,** *95*, 6341-6346.
28. Wang, L.; Liu, H.; Liu, Y.; Chen, Y.; Yang, S., Influence of preparation method on performance of Ni-CeO2 catalysts for reverse water-gas shift reaction. *Journal of Rare Earths* **2013,** *31* (6), 559-564.
29. Vesselli, E.; Schweicher, J.; Bundhoo, A.; Frennet, A.; Kruse, N., Catalytic CO_2 Hydrogenation on Nickel : Novel Insight by Chemical Transient Kinetics. *The Journal of Physical Chemistry C* **2011,** *115*, 1255-1260.
30. Goguet, A.; Meunier, F. C.; Tibiletti, D.; Breen, J. P.; Burch, R., Spectrokinetic Investigation of Reverse Water-Gas-Shift Reaction Intermediates over a Pt/CeO_2 Catalyst. *The Journal of Physical Chemistry B* **2004,** *108*, 20240–20246.
31. Campbell, T. K.; Falconer, J. L., Carbon dioxide hydrogenation on potassiumpromoted nickel catalysts. *Applied Catalysis* **1989,** *50* (1), 189-197.
32. Antolini, E.; Salgado, J. R. C.; Gonzalez, E. R., The methanol oxidation reaction on platinum alloys with the first row transition metals. *Applied Catalysis B: Environmental* **2006,** *63* (1-2), 137-149.
33. Isaifan, R. J.; Ntais, S.; Baranova, E. A., Particle size effect on catalytic activity of carbon-supported Pt nanoparticles for complete ethylene oxidation. *Applied Catalysis A: General* **2013,** *464-465*, 87-94.
34. Kim, S.; Park, K.; Hong, S. C., A study of the selectivity of the reverse water–gas-shift reaction over Pt/TiO2 catalysts. *Fuel Processing Technology* **2013,** *108*, 47-54.
35. Lee, J. S.; Oyama, S. T.; Boudart, M., Molybdenum Carbide Catalysts. *Journal of Catalysis* **1987,** *106*, 125-133.
36. Liao, L.; Bian, X.; Xiao, J.; Liu, B.; Scanlon, M. D.; Girault, H. H., Nanoporous molybdenum carbide wires as an active electrocatalyst towards the oxygen reduction reaction. *Physical chemistry chemical physics : PCCP* **2014,** *16* (21), 10088-10094.
37. (a) Xia, Y.; Yang, P.; Sun, Y.; Wu, Y.; Mayers, B.; Gates, B.; Yin, Y.; Kim, F.; Yan, H., One-Dimensional Nanostructures: Synthesis, Characterization, and

Applications. *Advanced materials* **2003,** *15*, 353-389; (b) Smalley, R. E., Future Global Energy Prosperity : The Terawatt Challenge. *Symp. X—Frontiers Mater. Res. Mater. Res. Soc. Fall Meet* **2004**.
38. Blank, H., Hägg's rule and fast solute diffusion in cubic transition-metal phases. *Philosophical Magazine Part B* **1996,** *73* (5), 833-844.
39. Wan, C.; Regmi, Y. N.; Leonard, B. M., Multiple phases of molybdenum carbide as electrocatalysts for the hydrogen evolution reaction. *Angewandte Chemie* **2014,** *53* (25), 6407-6410.
40. Katsuhiko, O.; Masatoshi, N.; Shinzo, O., Characterization of Molybdenum Carbides for Methane Reforming by TPR, XRD, and XPS. *The Journal of Physical Chemistry B* **2001,** *105*, 9124-9131.
41. Li, Z.; Chen, C.; Zhan, E.; Ta, N.; Li, Y.; Shen, W., Crystal-phase control of molybdenum carbide nanobelts for dehydrogenation of benzyl alcohol. *Chemical communications* **2014,** *50* (34), 4469-4471.
42. Xu, W.; Ramirez, P. J.; Stacchiola, D.; Rodriguez, J. A., Synthesis of α-MoC1-x and β-MoCy Catalysts for CO2 Hydrogenation by Thermal Carburization of Mo-oxide in Hydrocarbon and Hydrogen Mixtures. *Catalysis Letters* **2014,** *144* (8), 1418-1424.
43. Ricardo B. Levy, 4 - Properties of Carbides, Nitrides, and Borides: Implications for Catalysis. *Advanced Materials in Catalysis* **1977**, 101-127.
44. Xiao, T., Preparation of Nickel–Tungsten Bimetallic Carbide Catalysts. *Journal of Catalysis* **2002,** *209* (2), 318-330.
45. Chen, J.; Wang, M.; Liao, X.; Liu, Z.; Zhang, J.; Ding, L.; Gao, L.; Li, Y., Large-scale synthesis of single-crystal molybdenum trioxide nanobelts by hot-wire chemical vapour deposition. *Journal of Alloys and Compounds* **2015,** *619*, 406-410.
46. Gao, Q.; Zhang, C.; Xie, S.; Hua, W.; Zhang, Y.; Ren, N.; Xu, H.; Tang, Y., Synthesis of Nanoporous Molybdenum Carbide Nanowires Based on Organic−Inorganic Hybrid Nanocomposites with Sub-Nanometer Periodic Structures. *Chemistry of Materials* **2009,** *21* (23), 5560-5562.
47. Ma, Y.; Guan, G.; Phanthong, P.; Li, X.; Cao, J.; Hao, X.; Wang, Z.; Abudula, A., Steam reforming of methanol for hydrogen production over nanostructured wire-like molybdenum carbide catalyst. *International Journal of Hydrogen Energy* **2014,** *39* (33), 18803-18811.
48. Ping, L.; Jose´, A. R., Water-Gas-Shift Reaction on Molybdenum Carbide Surfaces: Essential Role of the Oxycarbide. *J. Phys. Chem. B* **2006,** *110* (39), 19418-19425.